

Article

Processing of Gypsum Construction and Demolition Waste and Properties of Secondary Gypsum Binder

Girts Bumanis , Jelizaveta Zorica , Aleksandrs Korjakin  * and Diana Bajare 

Department of Building Materials and Products, Riga Technical University, LV-1658 Riga, Latvia;
girts.bumanis@rtu.lv (G.B.); jelizaveta.zorica@rtu.lv (J.Z.); diana.bajare@rtu.lv (D.B.)

* Correspondence: aleksandrs.korjakin@rtu.lv

Abstract: The waste amount coming from construction and demolition (CDW) has significant volume and potential to provide the backbone of a secondary material bank. Up to now, little attention is paid to waste gypsum recycling from CDW while a shift in global attitude toward waste management brings motivation to use CDW gypsum as secondary raw material. The present research investigates the properties of gypsum binder obtained from secondary raw materials originating from CDW. Three types of drywall boards and cast monolithic gypsum from interior walls, treated in the laboratory, and a gypsum binder was obtained. Comparison has been studied and the most effective solutions regarding CDW treatment are represented. Separation, crushing, and milling were done. DTA/TG, XRD, SEM, and particle size distribution were characterized by CDW gypsum. The heat treatment temperature was selected at 130 °C for 4 or 24 h and 180 °C for 4 h. Consistency, set time, and mechanical properties were characterized. Results indicate that a gypsum binder with a strength up to 3.7 MPa can be obtained. Low strength is associated with fineness of CDW gypsum and a high water/gypsum ratio (from 0.6 to 1.396). Gypsum content in CDW (38 to 92 wt.%) should be considered as an important factor during gypsum CDW recycling.

Keywords: CDW; gypsum; recycling; binder; properties



Citation: Bumanis, G.; Zorica, J.; Korjakin, A.; Bajare, D. Processing of Gypsum Construction and Demolition Waste and Properties of Secondary Gypsum Binder. *Recycling* **2022**, *7*, 30. <https://doi.org/10.3390/recycling7030030>

Academic Editors: Elena Magaril, Elena Rada, Marco Ragazzi, Ioannis Katsoyiannis, Paolo Viotti, Hussain H. Al-Kayiem, Marco Schiavon, Gabriela Ionescu and Natalia Sliusar

Received: 13 April 2022

Accepted: 13 May 2022

Published: 17 May 2022

Publisher's Note: MDPI stays neutral with regard to jurisdictional claims in published maps and institutional affiliations.



Copyright: © 2022 by the authors. Licensee MDPI, Basel, Switzerland. This article is an open access article distributed under the terms and conditions of the Creative Commons Attribution (CC BY) license (<https://creativecommons.org/licenses/by/4.0/>).

1. Introduction

The gypsum industry is responsible for around 1% of the total amount of construction and demolition waste (CDW). It was estimated that every detached house with an area of 186 m² on average contains 1021 kg of gypsum drywall with a potential to become a CDW [1]. If gypsum CDW is disposed of in landfills, the production of hydrogen sulfide (H₂S) gas from the anaerobic degradation of gypsum residues can occur and bring environmental concerns [2]. Therefore, the recycling of gypsum CDW is within the scope of society.

In general, gypsum waste is categorized into three parts: waste coming from production, waste remaining during construction, and waste after the demolition of a building. The CDW waste is the most complex to recycle as gypsum is often combined with other building materials; therefore, its recycling efficiency is reduced. The target value of CDW gypsum recycling set up by EU-27 member states is 70% [3]. Up to now, plasterboard CDW can be separated and collected on-site, and when it is processed, from 20 to 30% of recycled gypsum can be used in the production of new plasterboards. In the year 2019, up to 600,000 t of recycled gypsum is used in the production of plasterboard [4]. CDW gypsum traditionally is characterized by high gypsum content, while some waste can contain mineral, organic, or fibrous fillers previously used in production [5].

In Denmark, the gypsum recycling industry has developed a recycling system where after crushing and screening three fractions of gypsum, paper and metal are obtained [6]. In a such way, the gypsum CDW can be used as secondary raw material and it is aimed to substitute above 30% of natural gypsum in the production of plasterboards [7]. Suárez et al.

concluded that 65% less energy is needed for recycled gypsum compared to natural ones [8]. An environmental impact evaluation shows that the utilization of recycled gypsum brings advantages even compared to coal-fired power plants (FGD) gypsum and also natural gypsum; however, it was concluded that the specific transportation distance has a great effect on the results [9].

Several studies have been published with the investigation of CDW gypsum as secondary gypsum material. The main parameters studied focused on the calcination process, temperature, and treatment time, in particular. Typical heat treatment temperatures of CDW gypsum were from 120 to 200 °C [10–12]. The properties of recycled gypsum from gypsum plasterboards after up to five recycling cycles were investigated by Erbs et al. showing the feasibility of gypsum recycling technology [13]. Other test reports showed that the reversibility of gypsum hydration enabled the generation of recycled gypsum in three cycles without losses in the building material properties [9]. It was determined, that the recycled gypsum material particles are smaller than the commercial sample, which was confirmed by fineness modulus, particle size distribution, and specific surface area, which is almost 17% higher than the recycled sample [11]. Recycled gypsum plaster with 80% particles finer than 0.297 mm showed compression strength of 8.4 MPa at a heat treatment temperature of 150 °C with a water/gypsum ratio up to 0.8 [12]. The gypsum CDW recycling efficiency is still being investigated and evaluated to reach the highest efficiency of a closed life-cycle loop of gypsum binder.

The properties of gypsum binders coming from four types of CDW have been investigated in this research. The recycling process and the properties of the secondary gypsum binder were determined. The effect of heat treatment was investigated on the properties of the binder obtained from CDW.

2. Materials and Methods

Gypsum CDW was collected directly from different running construction sites. Both demolished gypsum waste and remains from construction from new drywall mounting were collected. Three drywall types were identified—gypsum drywall, impregnated (Type H); gypsum drywall, fire-resistant (Type H); gypsum drywall, standard (Type A)—and one demolished gypsum monolithic wall (MG) from the construction site sample was obtained. CDW gypsum was compared to a commercial gypsum (CG). Monolith gypsum contained sand filler and wooden chips as reinforcement. Materials were further processed in the laboratory. Air-dry gypsum CDW was processed in a jaw crusher to remove the paper and to obtain gypsum CDW gravel (<11.2 mm) used for further grinding (Figure 1). Then gypsum CDW was milled to powder-like particles by collision milling in a semi-industrial disintegrator with a rotational speed of 50 Hz [14]. The obtained gypsum powder was used for further research as a secondary gypsum binder.

For CDW gypsum powder, the particle size distribution was determined by sieving 10 g of CDW gypsum through 0.5 mm, 0.355 mm, and 0.125 mm sieves to remove large particles (remaining paper, synthetic fibers, and wood chips) and sieved powder (0.5 g) was analyzed with the laser diffraction analysis instrument Analysette 22 NanoTec (FRITSCH GmbH). FTIR spectra of CDW gypsum were detected using a Varian 800 FT-IR Smicitar Series spectrometer. KBr method was used for scanning. Samples were prepared using 3 mg of CDW gypsum with 300 mg KBr ground together for 1 min, and then test tablets (d13 mm) were pressed with a uniaxial force of 50 kN. The infrared spectra were recorded in the range of 4000–400 cm⁻¹. XRD was determined with PANalytical X'pert PRO. XRD parameters were 2θ 0.001°, 40 kV, and 30 mA, with a scanning range from 10–80°. Peaks were analyzed using X'pert highscore software. Thermogravimetric analysis (TGA) was used to analyze the thermal behavior of the CDW gypsum samples. TGA was performed using a SETSYS Evolution TGA-DTA/TMA SETARAM instrument. A 15–20 mg of sample was placed in a platinum pan and heated in a nitrogen atmosphere from 25 °C to 1050 °C at 10 °C/min in the same gas environment. Mettler Toledo STARe Thermal Analysis Excellence System Software was used for result analysis. The macro and microstructure of CDW gypsum were

observed by using a scanning electron microscope (TESCAN Mira/LMU Field-Emission-Gun, Kohoutovice, Czech Republic).



Figure 1. The treatment process of CDW to obtain secondary gypsum powder for binder production: (a) collection of gypsum wallboard CDW; (b) crushing of wallboards with laboratory jaw crusher; (c) gypsum CDW aggregate ($<11.2\text{ mm}$) prepared for milling; (d) gypsum CDW milling in disintegrator (collision milling).

Gypsum content in CDW samples was determined by the gypsum dehydration method described in the literature [15]. Removal of free water from gypsum was performed at 45°C . As the temperature continues to increase above 45°C , the gypsum turns to hemihydrate, and at about 100°C , all the hydration water is lost and the material becomes anhydrite, CaSO_4 . As the ratio of the weight of hydration water to the weight of gypsum is known as 0.2093, the amount of gypsum may be found by multiplying the weight of hydration water by the inverse of this ratio, i.e., 4.7778. The weight of a specimen was recorded before it was put in the drying chamber at 45°C , and then after high-temperature treatment (130 or 180°C). The weight of hydration water will be the difference between the weights of the specimen at the two different temperatures.

Accordingly, the gypsum content may be determined as:

$$X = \frac{W_{45^\circ\text{C}} - W_{130/180^\circ\text{C}}}{W_{45^\circ\text{C}}} \times 4.7778 \times 100 \quad (1)$$

where

X is the gypsum content, percentage of solids.

$W_{45^\circ\text{C}}$ is the weight of solids at 45°C .

$W_{130/180^\circ\text{C}}$ is the weight of solids at 130 or 180°C .

In this study, a secondary CDW gypsum binder was prepared according to the DTA/TG results and literature. The heating of disintegrated gypsum CDW was performed in a heating chamber under the following conditions: 4 h at 180°C temperature; 4 h at 130°C temperature, and 24 h at 130°C temperature (Table 1). The 130°C temperature was selected as all CDW gypsum types showed endothermic peak between 125 and 133°C .

Then, the technological properties of the obtained binder were tested. The water requirement of normal consistency for gypsum plaster is the water/powder ratio when the fluidity of the paste is in the range of $180\text{ mm} \pm 5\text{ mm}$ testing by stainless steel cylinder with a height of 100 mm and an inner diameter of 50 mm . The setting time of gypsum plaster at normal consistency was measured by the Vicat apparatus. A group of nine cubical specimens of size $20 \times 20 \times 20\text{ mm}^3$ was prepared for determination of the compressive strength.

Table 1. Treatment parameters of CDW gypsum to obtain secondary binder.

CDW Waste Type	Treatment Temperature and Duration		
	130 °C	130 °C	180 °C
Type A			
Type H	4 h		
Type F		24 h	
Monolithic gypsum (MG)			4 h

3. Results

XRD patterns of CDW gypsum are given in Figure 2. Similarities between Type A and Type F can be observed as practically identical XRD patterns were obtained. Besides gypsum (Ref # 021-0816) peaks, XRD peaks of the dolomite (ref# 036-0426) were observed for both types of CDW, which could indicate some content of aggregates or additives to control gypsum pH and compatibility with other building materials used in construction. In Type H, no aggregate phase was observed and only gypsum peaks were dominant. In MG, there were constituents of dolomite and gismondine (Ref# 020-0452) as indicated with XRD. Dolomite is a natural component of sand used in building materials. Gismondine is a calcium aluminum silicate hydrate that may form in high aluminosilicate compositions and persists in the presence of calcite, and gypsum [16]. Gismondine can give additional strength to the material [17].

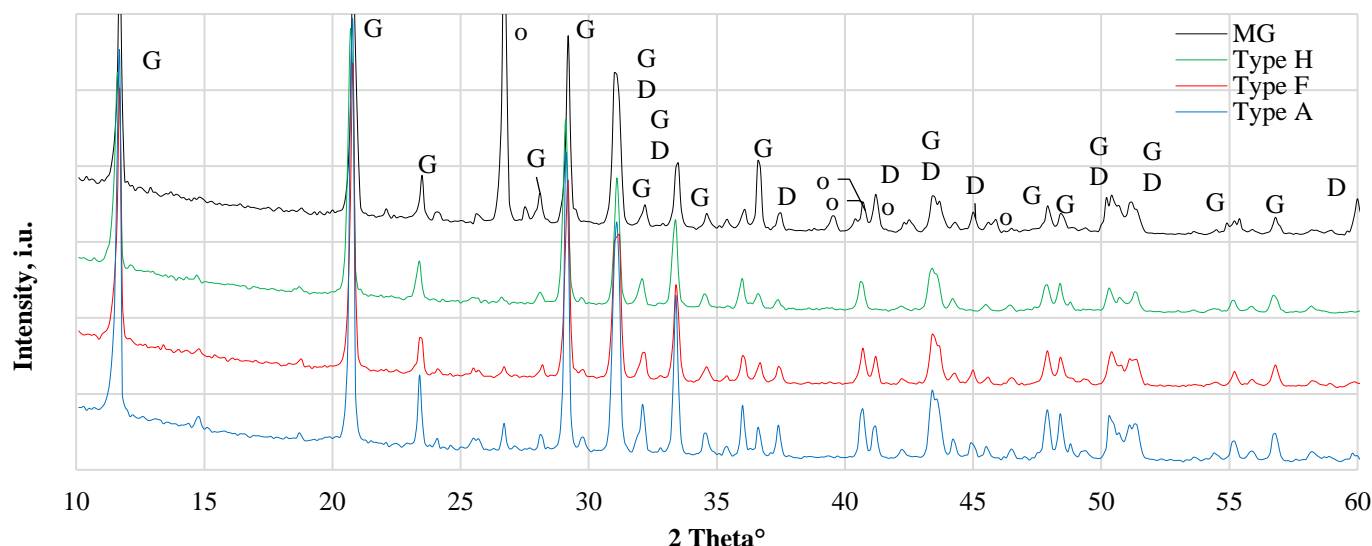


Figure 2. XRD results of different types of gypsum CDW. MG—gypsum monolithic wall CDW; Type H—gypsum drywall, impregnated; Type F—gypsum drywall, fire-resistant; Type A—gypsum drywall, standard. G—gypsum $\text{CaSO}_4 \cdot 2\text{H}_2\text{O}$, ref# 021-0816, D—Dolomite, $\text{CaMg}(\text{CO}_3)_2$, ref# 036-0426, o—Gismondine, $\text{CaAl}_2\text{Si}_2\text{O}_8 \cdot 4\text{H}_2\text{O}$, ref# 020-0452.

FTIR results of CDW gypsum are given in Figure 3. Also, all FTIR patterns seem similar as the main component in CDW is gypsum, a noticeable difference was detected for Type H. Type H did not absorb wavelength at 879 and 1453 cm^{-1} while other gypsum CDW had this absorbance. The presence of the C–O stretching mode of carbonate with a strong band at 1453 cm^{-1} together with the bending mode band at 873 cm^{-1} indicates the presence of carbonates (calcite CaCO_3 or dolomite $\text{CaCO}_3 \cdot \text{MgCO}_3$). A similar observation previously was detected for the investigation of the ternary mixture of calcium carbonate (CaCO_3), calcium sulfate hemihydrates ($\text{CaSO}_3 \cdot 1/2\text{H}_2\text{O}$), and gypsum ($\text{CaSO}_4 \cdot 2\text{H}_2\text{O}$) by FTIR spectroscopy [18,19]. Bands at 980 and 652 cm^{-1} are associated with sulfate ions while H_2O stretching vibrations are observed at 3402 and 3527 cm^{-1} and H_2O bending at

1620 and 1683 cm^{-1} . Vibrations bands of the SO_4^{2-} anion are located at 595 and 660 cm^{-1} . Absorption at 1004 , 1112 cm^{-1} is attributed to basanite $2\text{CaSO}_4 \cdot \text{H}_2\text{O}$ [20].

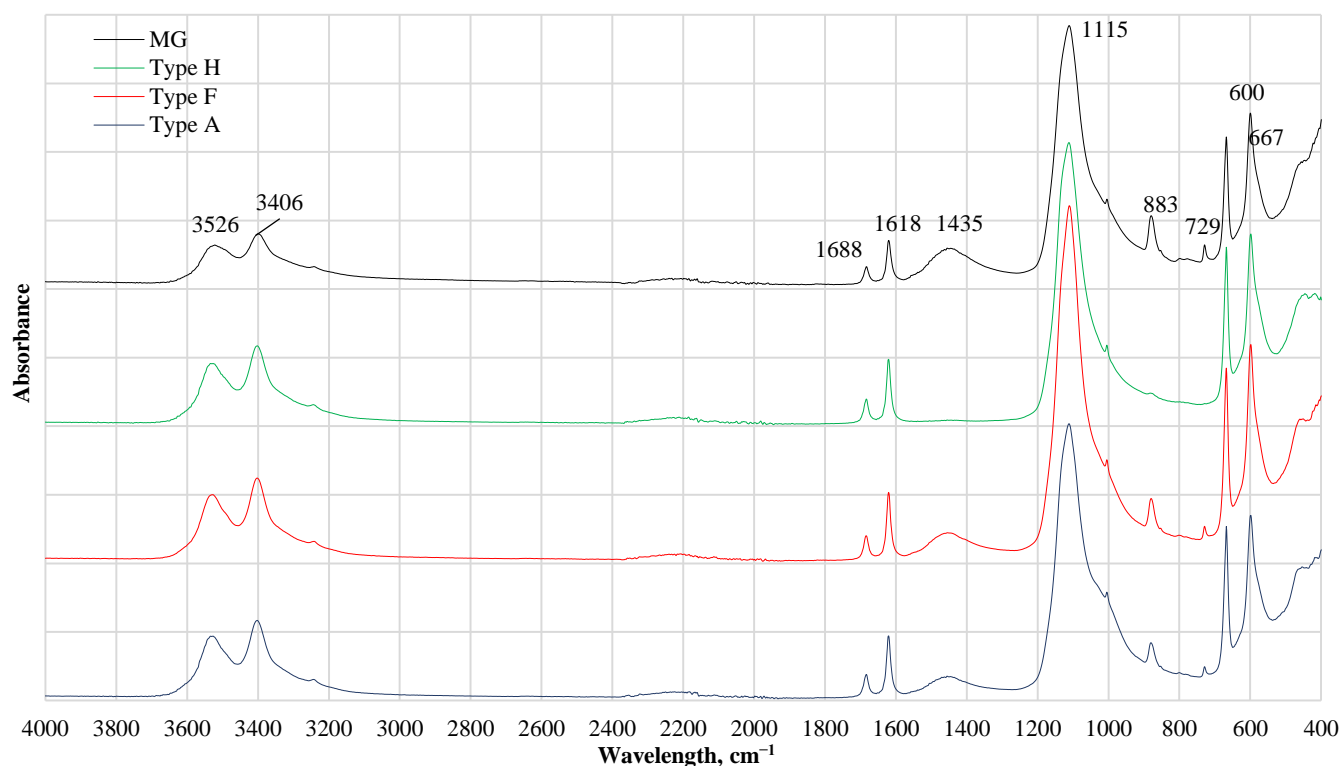


Figure 3. FTIR results of different types of gypsum CDW. MG—gypsum monolithic wall CDW; Type H—gypsum drywall, impregnated; Type F—gypsum drywall, fire-resistant; Type A—gypsum drywall, standard.

DTA/TG results are given in Figure 4. The curves show two consecutive and much closed endothermic peaks between $128.5\text{ }^\circ\text{C}$ and $144.6\text{ }^\circ\text{C}$ when 15.6 wt.% mass loss is detected. This trend is traditional to gypsum binder to produce hemihydrate gypsum and the second peak to the transformation of hemihydrate to anhydrite [21]. Then, from 610.8 to $733.2\text{ }^\circ\text{C}$ with a peak at $712.4\text{ }^\circ\text{C}$, another endothermic effect was observed. The peak at around $700\text{ }^\circ\text{C}$ was found to correspond to the decomposition of CaCO_3 [22]. It was associated with an additional 8 wt.% mass loss. A similar trend was observed for Type F with endothermic peaks at $130\text{ }^\circ\text{C}$ and $144\text{ }^\circ\text{C}$. 14.6 wt.% mass loss was after the first two transformations, and the final mass loss was 25.6 wt.% (above $730\text{ }^\circ\text{C}$). MG had the first two transformations at $125.2\text{ }^\circ\text{C}$ and $136\text{ }^\circ\text{C}$ with weight loss of 6.6 wt.%, and 16.6 wt.% loss was above $740.8\text{ }^\circ\text{C}$. The peak intensities and weight loss indicate low gypsum content in the material and an increased amount of calcareous and inert aggregates. Different DTA/TG results were observed for Type H as it shows only the first two endothermic peaks at 132.8 and $148\text{ }^\circ\text{C}$. At $132.8\text{ }^\circ\text{C}$, weight loss was 9.85%, and after the second transformation, it reached 18.85 wt.%. This correlates well with FTIR data and gypsum content data as no additional decomposition of elements was observed. All of the specimens exhibited the thermal and gravimetric profiles typical of calcium sulfate dihydrate decomposition while crystal reordering at around $500\text{ }^\circ\text{C}$ was not detected as previously, it was determined that some changes in DTA or TGA may not be evident because they are too small to identify [23].

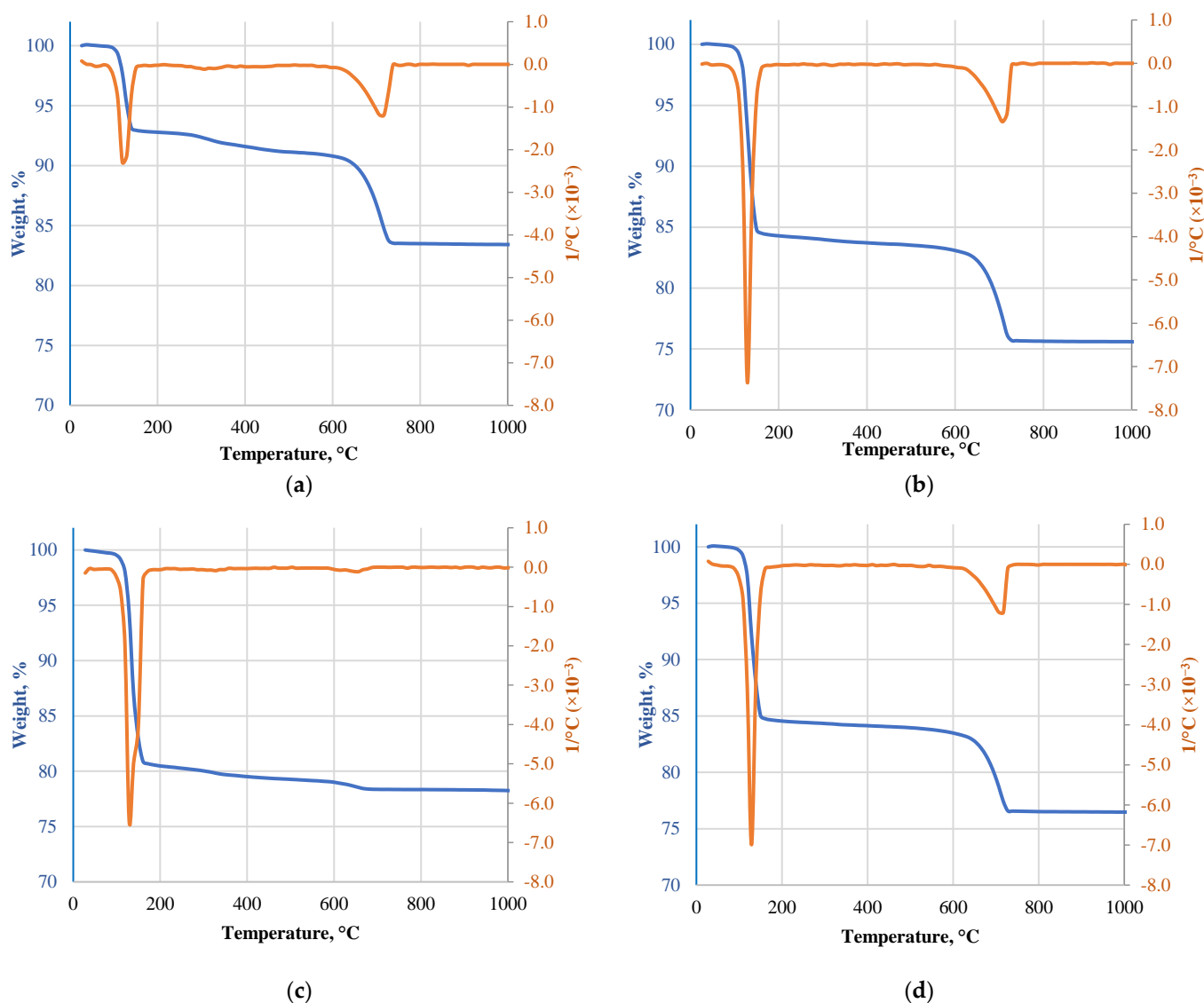


Figure 4. DTA/TG results of different types of gypsum CDW: (a) MG; (b) Type F; (c) Type H; (d) Type A.

Ground CDW plasterboards were sieved through a 0.5 mm sieve and 3, 4, and 6 wt.% of total particles remained, respectively. Higher remaining content for Type H and Type F was associated with higher glass fiber content in plasterboard to obtain higher bearing or fire resistance capacity. Fine gypsum powder was obtained with applied grinding parameters, and sieved powder was analyzed with a laser diffraction analysis instrument. Sieving of MG through 0.5 mm, 0.355 mm, and 0.125 mm indicated that 5 wt.%, 4 wt.%, and 29 wt.% making it 37 wt.% of particles >0.125 mm. MG had a different production method as it was intended as monolithic wall material. Sand and wood fibers were detected in MG composition. Grinding effectively ground mineral particles while wood fibers remained coarse. This had a significant influence on the gypsum content and technological properties of obtained binder from MG CDW. Laser diffraction analysis indicates that all CDW gypsum types were finer compared to commercial gypsum reference (CG) (Figure 5). The finest gypsum powder was obtained from Type A and Type F drywall while MG and Type H remained coarser. MG has harder sand particles, which need more energy to grind to finer particles, while Type H drywall use impregnation materials to increase moisture resistance of drywall and may affect grinding parameters [14]. The particle size characterization given in Table 2 supports the fact that Type A has finer particles. d_{10} was

0.021, 0.027, 3.7, and 22 μm ; d_{50} was 0.078, 0.122, 24.9, and 118 μm ; and d_{90} was 8, 13, 88, and 210 μm for Type A, Type F, MG, and Type H, respectively. Similar characteristics were observed for Type A and Type F drywall. It was assumed that the main difference between Type A and Type F is fiber content and initial density of gypsum CDW, as well as different properties of lining paper to improve Type F fire performance.

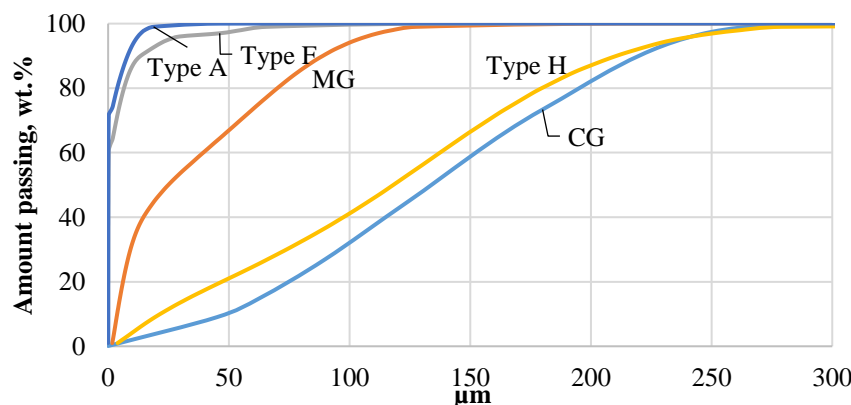


Figure 5. Particle size distribution of different types of gypsum CDW determined by laser diffraction analysis: Type A—white standard plasterboard; Type H—Impregnated gypsum plasterboard; Type F—fire-resistant plasterboard; MG—monolithic gypsum wall CDW; CG—commercial gypsum.

Table 2. Particle size characterization of gypsum CDW.

Sample	d_{10} , μm	d_{50} , μm	d_{90} , μm
MG	3.7 ± 0.3	24.9 ± 9.6	88 ± 8
Type F	0.027 ± 0.001	0.122 ± 0.003	13 ± 5
Type H	22 ± 8	118 ± 11	210 ± 6
Type A	0.021 ± 0.001	0.078 ± 0.001	8.0 ± 0.3

The weight loss of CDW gypsum after heating was expected to be approximately 15%, which would indicate that dihydrate transformed to hemihydrate. Additionally, adsorbed water could increase this value, while heating at 45 °C should remove free water. The weight loss after heating 4 h at 180 °C temperature was around 16 ± 2%, except for MG, which was 7.7%. The heating at the lower temperature of 130 °C for 4 h resulted in very close results as for 180 °C heating, and the difference was not more than 0.4%. The longer heating time of 24 h at the 130 °C enlarged weight loss up to 22.3% for Type H, but for MG, it was the lowest of 9.4%. The difference between the weight loss of specimens is thought to be explained by the percentage of gypsum in the material [15]. By the results given in Table 3, the highest dosage of gypsum had Type H (91.92%), Type F and Type A had gypsum content from 74.78 to 75.68%, and the lowest value had MG (38.22%), which appeared to be true as MG has plenty of wood chips and sand in the composition, and this corresponds well to the results obtained from XRD, FTIR, and particle size analysis.

Table 3. Weight loss after heating and calculated gypsum content.

	Weight Loss, %			
	MG	Type F	Type H	Type A
45 °C	0.07	0.03	0.13	0.03
4 h at 130 °C	8.1	14.9	18.1	14.9
24 h at 130 °C	9.4	17.0	22.3	17.6
4 h at 180 °C	7.7	15.1	18.2	14.7
DTA/TG *	5.0–7.2	7.0–15.6	5.7–19.4	7.9–15.4
Gypsum content, %	38.22	74.78	91.92	75.68

* weight loss was taken at 130 and 180 °C.

3.1. Microstructural Investigation

SEM Analysis

The morphology of CDW gypsum crystals is given in Figure 6. Figure 6a–d are assigned to untreated CDW gypsum powder, while Figure 6e–h are assigned to heat treated gypsum at 180 °C for 4 h. The Basanite-type crystal morphology was detected for all CDW types [24]. Such clusters are present in structures of all plasterboard source gypsum CDW. GW morphology is slightly different as smooth surface aggregate and filament particles are dominating in the structure of this type of CDW. Gypsum crystal traces can be detected on their surface. For MG CDW, aggregates and wood fibers were also detected in its structure. Crystals have the largest crystal cluster size up to 20 µm, which corresponds to the laser particle size distribution. Structure of CDW from plasterboard recycling had similar microstructure. For Type F, glass fibers were also detected. After heat treatment, the microstructure of gypsum CDW was practically identical.

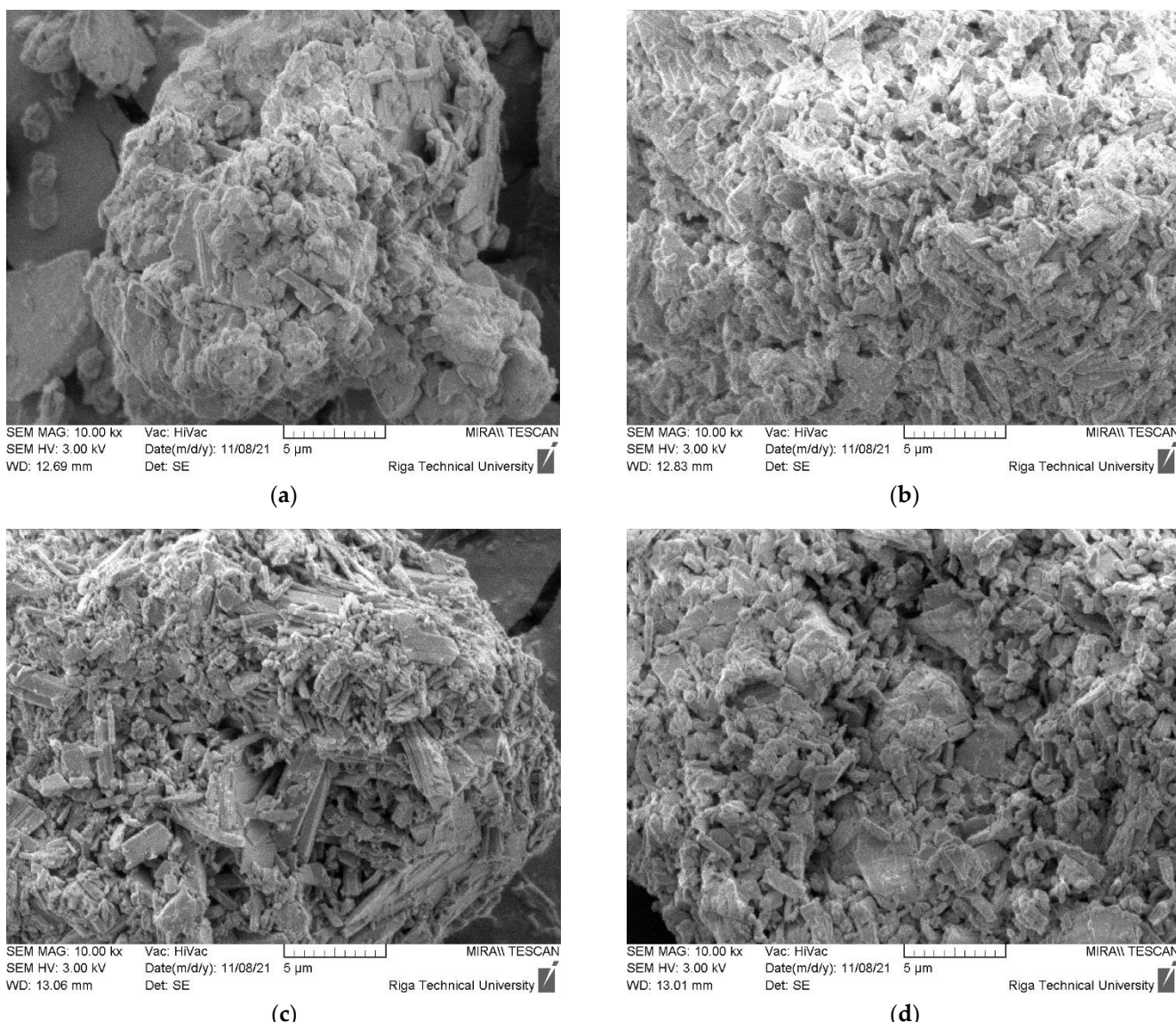


Figure 6. Cont.

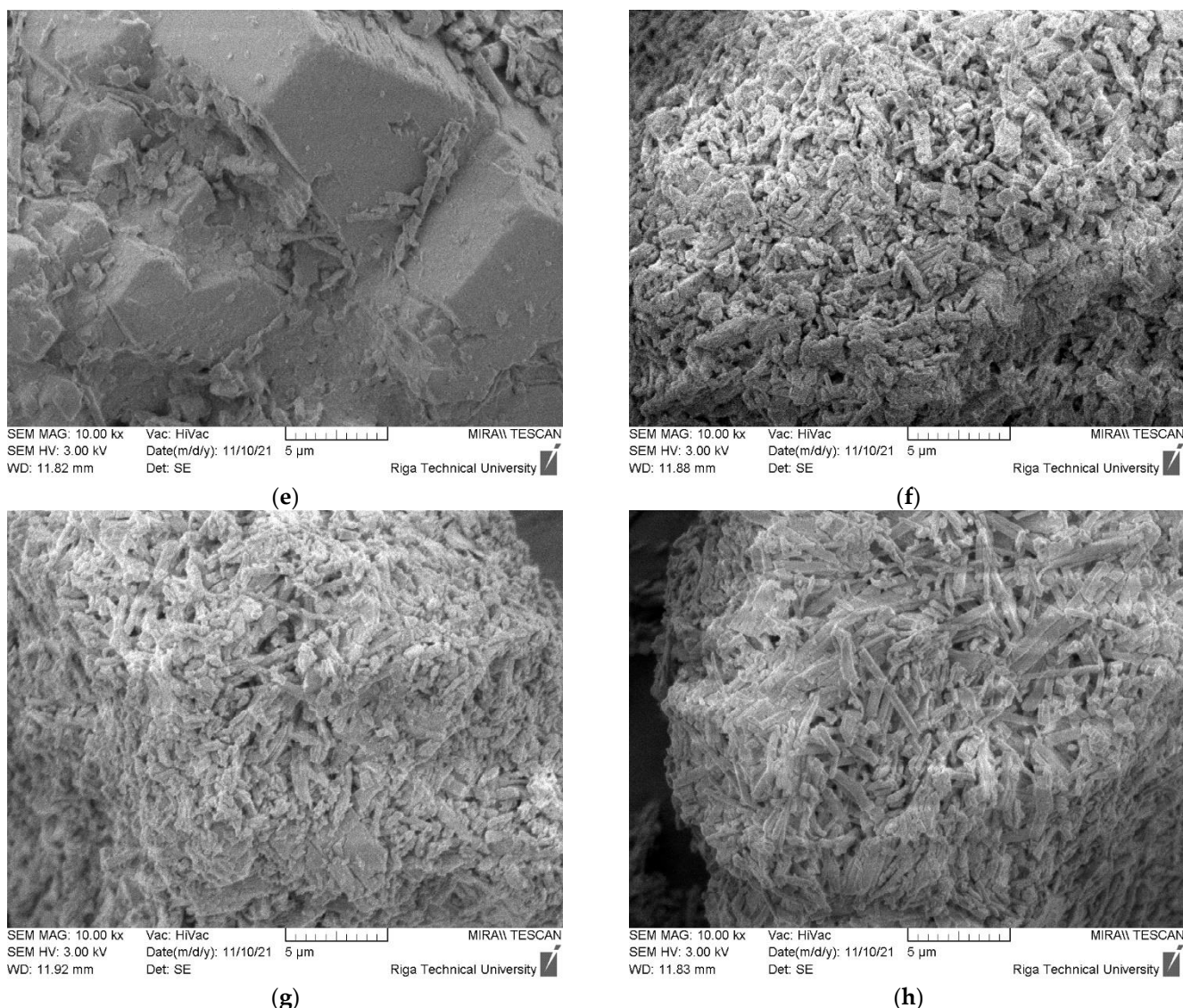


Figure 6. Morphology of CDW gypsum. (a–d) Untreated CDW gypsum; (e–h) heat treated at 180 °C for 4 h. (a,e) MG, (b,f) Type F, (c,g) Type H, (d,h) Type A.

3.2. Technological Properties of Secondary Gypsum Binder

Obtained secondary gypsum binder was tested on consistency, density, setting time, and strength. The standard consistency of Suttard ring flow at 180 mm was achieved and with such, W/B ratio properties of secondary gypsum binder tested. Results for CDW gypsum treated 4 h at 130 °C are given in Table 4. The W/B of standard consistency was relatively high in comparison to CG. For secondary gypsum binder based on plasterboard CDW, it was more than 1.0, except for MG with a result of 0.57. The most water-demanding binder was Type H with W/B of 1.35. The setting time of Type F was close to CG. Type H and Type A showed a similar initial set time of 35 and 40 min, and final time of 41 and 45 min, accordingly. The longest setting time was for MG, which started to set more than 60 min after mixing. Increased water demand could be contributed to the fine nature of gypsum powder, also the recycled and industrial gypsum has smaller crystals than the natural gypsum.

Table 4. Properties of commercial gypsum and CDW gypsum binder treated for 4 h at 130 °C.

Gypsum	W/B	Set Time, min		Density, kg/m ³	Compressive Strength, MPa		
		t _{init.}	t _{fin.}		2 h	7 Days	28 Days
CG	0.450	10	17	1340	5.8	12.9	13.2
MG	0.570	78	85	1054	0.6	1.4	1.3
Type F	1.025	20	26	804	1.0	2.9	2.7
Type H	1.350	16	19	621	0.7	2.1	1.6
Type A	1.048	24	27	804	1.0	2.8	2.7

The dry density of Type F and Type A was $800 \pm 5 \text{ kg/m}^3$ and the compressive strength was the highest compared to other waste gypsum binders observed in the Table 4, with 4.40 and 2.36 MPa, accordingly, after 7 days. The density obtained was similar as given for plasterboards. The compressive strength of MG and Type H after 7 days is close to 1.0 MPa, although the density was significantly different (1096 and 583 kg/m^3). MG has a high content of mineral aggregates, which indicates low water demand during mixing, and this resulted in increased density. Low gypsum content contributed to the reduced strength as well. The appearance of gypsum samples indicated that Type H was white, while MG was grey to brown indicating the addition of mineral fillers. The low-density gypsum samples prepared from Type H CDW could be associated with its chemical composition and admixtures, to be more precise. During the initial production, superplasticizers (PCE), stability controlling admixtures, set retarders, and accelerators, as well as water retaining admixtures, remains in the plasterboard composition and, after its recycling, they might react as air entraining admixtures, thus summarizing in reduced density of gypsum samples.

The heating parameter change to 130 °C for 24 h did not affect the properties of the secondary binder (Table 5). The setting time of the binder was slightly shorter in some cases but a significant difference was not observed. The compressive strength tended to increase slightly and reached 3.1 MPa for Type F gypsum at 28 days.

Table 5. Properties of commercial gypsum and CDW gypsum binder treated for 24 h at 130 °C.

Gypsum	W/B	Set Time, min		Density at 7 Days, kg/m ³	Compressive Strength, MPa		
		t _{init.}	t _{fin.}		2 h	7 Days	28 Days
CG	0.450	10	17	1340	5.8	12.9	13.2
MG	0.570	58	69	1083	0.6	1.4	1.2
Type F	1.025	18	23	796	1.2	3.2	3.1
Type H	1.350	15	19	575	0.6	1.6	1.3
Type A	1.048	26	29	813	0.9	2.3	2.2

The W/B ratio and the dry density for gypsum dried at 130 °C for 24 h were the same as for dried at 180 °C for 4 h (Table 6). The setting time was very close to the gypsum dried at the same temperature for 4 h. The compressive strength for gypsum treated at a higher temperature slightly decreased and reached 2.4 MPa for Type A binder at 28 days. The results indicate that higher heating temperature can even reduce the strength of gypsum binder.

The comparison of compressive strength results is given in Figure 7. The early strength at 2 h after mixing shows strength from 0.4 to 1.5 MPa. The lowest strength was for binders obtained from gypsum walls. It is associated with the lowest gypsum content in the compositions. The highest result was for Type F. Since the composition of Type F binder was similar to Type A, the difference in strength could be explained by additives present in gypsum structure from the previous production (e.g., fibers, densifiers). At the age of 28 d, the strength increased from 1.0 to 3.1 MPa. MG showed the lowest strength (1.2–1.3 MPa), while Type A and Type F gypsum showed strength from 2.2 to 3.1 MPa. The low strength

for Type H is associated with the low density, which could be related to the highly porous structure of gypsum. The optimal heating conditions identified were 130 °C for 24 h.

Table 6. Properties of commercial gypsum and CDW gypsum binder treated for 4 h at 180 °C.

Gypsum	W/B	Set Time, min		Density at 7 Days, kg/m ³	Compressive Strength, MPa		
		t _{init.}	t _{fin.}		2 h	7 Days	28 Days
CG	0.450	10	17	1340	5.8	12.9	13.2
MG	0.570	≥60	88	1096	0.4	1.0	1.2
Type F	1.025	14	16	804	1.5	1.6	1.6
Type H	1.350	35	41	583	0.4	0.9	1.0
Type A	1.050	40	45	796	0.8	2.3	2.4

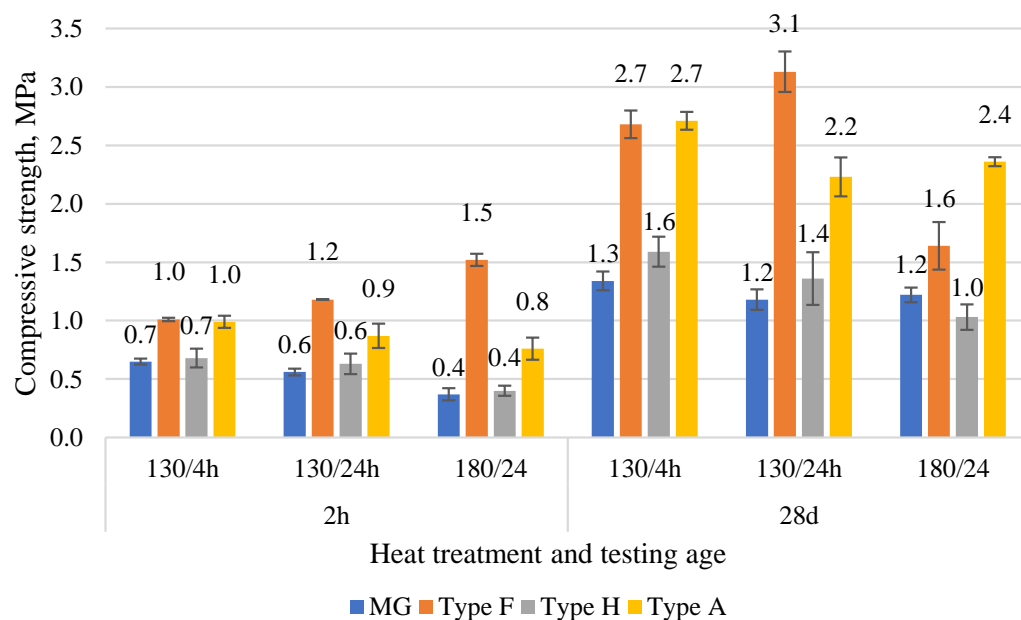


Figure 7. The compressive strength of various CDW gypsum binders was obtained in three different temperature regimes at the age of 2 h and 28 d.

4. Conclusions

Research showed the perspective of different gypsum construction and demolition waste type application for the production of secondary gypsum binders. The three most common plasterboard types and monolithic gypsum walls proved to be suitable for the production of gypsum binder. Results indicated that gypsum content in the secondary binder can vary from 38 to 92%. The mineral aggregates, as well as wood and glass fibers, were detected. The DTA/TG results indicate that the most optimal heating temperature to obtain gypsum hemihydrate is 130 °C. The particle size distribution showed fine characteristics of the binder, which resulted in high water demand to reach the standard consistency of the binder. Cured specimens were characterized by low density, especially for binder based on impregnated plasterboard gypsum (575 kg/m³). All samples had strength from 0.4 to 1.5 MPa at an early age (2 h), while the final strength at the age of 14 d was from 1.0 to 3.1 MPa. As compared to the strength results, the most optimal heating condition was 130 °C for 4 h, which correlates well with DTA/TG results. This gives an optimistic result as there is no need to apply high temperatures (180 °C) and prolonged heating time. Present research proved that it is possible to obtain gypsum binder from CDW gypsum, while obtained strength results were low (1.0–3.1 MPa), which could be a problem associated with circular production. Partial replacement of natural gypsum binder could solve the problem and allow to obtain binder with higher strength.

Author Contributions: Conceptualization, G.B., D.B. and A.K.; methodology, G.B. and D.B.; validation, G.B., J.Z., D.B. and A.K.; formal analysis, G.B.; investigation, G.B. and J.Z.; resources, G.B. and D.B.; data curation, G.B. and J.Z.; writing—original draft preparation, G.B. and J.Z.; writing—review and editing, G.B., J.Z., D.B. and A.K.; visualization, G.B. and J.Z.; supervision, G.B., D.B. and A.K.; project administration, G.B. and D.B.; funding acquisition, G.B. and D.B. All authors have read and agreed to the published version of the manuscript.

Funding: This research was funded by the FLPP (Fundamental and Applied Research Projects) Programme in Latvia under the research project LZP-2020/1-0010 “Reuse of gypsum and expanded polymers from construction and demolition waste for acoustic and thermal insulation panels”.

Institutional Review Board Statement: Not applicable.

Informed Consent Statement: Not applicable.

Data Availability Statement: The data presented in this study are available on request from the corresponding author.

Conflicts of Interest: The authors declare no conflict of interest.

References

1. Pacheco-Torgal, F. Introduction to the recycling of construction and demolition waste (CDW). In *Handbook of Recycled Concrete and Demolition Waste*; Elsevier Inc.: Amsterdam, The Netherlands, 2013; pp. 1–6.
2. Yang, K.; Xu, Q.; Townsend, T.G.; Chadik, P.; Bitton, G.; Booth, M. Hydrogen sulfide generation in simulated construction and demolition debris landfills: Impact of waste composition. *J. Air Waste Manag. Assoc.* **2006**, *56*, 1130–1138. [CrossRef] [PubMed]
3. Eurogypsum-Association Européenne Des Industries du Plâtre. GtoG: From Production to Recycling, a Circular Economy for the European Gypsum Industry with the Demolition and Recycling Industry. Available online: https://webgate.ec.europa.eu/life/publicWebsite/index.cfm?fuseaction=search.dspPage&n_proj_id=4191 (accessed on 4 April 2022).
4. Jiménez-Rivero, A.; García-Navarro, J. Best practices for the management of end-of-life gypsum in a circular economy. *J. Clean. Prod.* **2017**, *167*, 1335–1344. [CrossRef]
5. Deloitte; BRE; ICEDD; RPS; VTT; University of Lisbon. Resource efficient use of mixed wastes improving management of construction and demolition waste. In Proceedings of the Workshop ‘Improving Management of Construction and Demolition Waste’, Brussels, Belgium, 25 May 2016.
6. ACA. ACA-Crusher for Recycling of Plasterboard and Production Waste. Available online: <https://www.environmental-expert.com/products/aca-crusher-for-recycling-of-plasterboard-and-production-waste-496806> (accessed on 16 February 2022).
7. Environmental Industry Companies. Available online: <https://www.environmental-expert.com/companies/gypsum-recycling-international-29016> (accessed on 16 February 2022).
8. Suárez, S.; Roca, X.; Gasso, S. Product-specific life cycle assessment of recycled gypsum as a replacement for natural gypsum in ordinary Portland cement: Application to the Spanish context. *J. Clean. Prod.* **2016**, *117*, 150–159. [CrossRef]
9. Weimann, K.; Adam, C.; Buchert, M.; Sutter, J. Environmental evaluation of gypsum plasterboard recycling. *Minerals* **2021**, *11*, 101. [CrossRef]
10. Ahmed, A.; Ugai, K.; Kamei, T. Investigation of recycled gypsum in conjunction with waste plastic trays for ground improvement. *Constr. Build. Mater.* **2011**, *25*, 208–217. [CrossRef]
11. Cordon, H.C.F.; Cagnoni, F.C.; Ferreira, F.F. Comparison of physical and mechanical properties of civil construction plaster and recycled waste gypsum from São Paulo, Brazil. *J. Build. Eng.* **2019**, *22*, 504–512. [CrossRef]
12. Camarini, G.; Lima, K.D.D.S.; Pinheiro, S.M.M. Investigation on gypsum plaster waste recycling: An eco-friendly material. *Green Mater.* **2015**, *3*, 104–112. [CrossRef]
13. Erbs, A.; Nagalli, A.; de Carvalho, K.Q.; Myrrin, V.; Passig, F.H.; Mazer, W. Properties of recycled gypsum from gypsum plasterboards and commercial gypsum throughout recycling cycles. *J. Clean. Prod.* **2018**, *183*, 1314–1322. [CrossRef]
14. Bumanis, G.; Goljandin, D.; Bajare, D. The Properties of Mineral Additives Obtained by Collision Milling in Disintegrator. *Key Eng. Mater.* **2016**, *721*, 327–331. [CrossRef]
15. Al-Mufty, A.; Hameed, I. Gypsum Content Determination in Gypseous Soils and Rocks. In Proceedings of the Third Jordanian International Mining Conference, Amman, Jordan, 25–28 April 2000.
16. Okoronkwo, M.U.; Mondal, S.K.; Wang, B.; Ma, H.; Kumar, A. Formation and stability of gismondine-type zeolite in cementitious systems. *J. Am. Ceram. Soc.* **2020**, *104*, 1513–1525. [CrossRef]
17. Thirumalini, S.; Sekar, S.K.; Bhuvaneshwari, B.; Iyer, N.R. Bio-inorganic composites as repair mortar for heritage structures. *J. Struct. Eng.* **2015**, *42*, 294–304.
18. Al Dabbas, M.; Eisa, M.Y.; Kadhim, W.H. Estimation of Gypsum-Calcite Percentages Using a Fourier Transform Infrared Spectrophotometer (FTIR), in Alexandria Gypsiferous Soil-Iraq. *Iraqi J. Sci.* **2014**, *55*, 1916–1926.
19. Böke, H.; Akkurt, S.; Özdemir, S.; Göktürk, E.H.; Caner Saltik, E.N. Quantification of $\text{CaCO}_3\text{-CaSO}_3\cdot 0.5\text{H}_2\text{O}\text{-CaSO}_4\cdot 2\text{H}_2\text{O}$ mixtures by FTIR analysis and its ANN model. *Mater. Lett.* **2004**, *58*, 723–726. [CrossRef]

20. Castro-Sastre, M.; Fernández-Abia, A.I.; Piep, J.; Rodríguez-González, P.; Barreiro, J. Towards Functional Parts by Binder Jetting Calcium-Sulphate with Thermal Treatment Post-Processing. *Materials* **2020**, *13*, 3818. [[CrossRef](#)] [[PubMed](#)]
21. López, F.A.; Tayibi, H.; García-Díaz, I.; Alguacil, F.J. Thermal dehydration kinetics of phosphogypsum. *Mater. Constr.* **2015**, *65*, e061. [[CrossRef](#)]
22. Wakili, K.G.; Hugi, E.; Wullschleger, L.; Frank, T. Gypsum Board in Fire—Modeling and Experimental Validation. *J. Fire Sci.* **2007**, *25*, 267–282. [[CrossRef](#)]
23. Engbrecht, D.C.; Hirschfeld, D.A. Thermal analysis of calcium sulfate dihydrate sources used to manufacture gypsum wallboard. *Thermochim. Acta* **2016**, *639*, 173–185. [[CrossRef](#)]
24. Rabizadeh, T.; Peacock, C.L.; Benning, L.G. Carboxylic acids: Effective inhibitors for calcium sulfate precipitation? *Mineral. Mag.* **2014**, *78*, 1465–1472. [[CrossRef](#)]